PHYSICAL REVIEW E **69**, 030201(R) (2004)

Superlensing effect in liquid surface waves

Xinhua Hu, Yifeng Shen, Xiaohan Liu, Rongtang Fu, and Jian Zi*
Surface Physics Laboratory (National Key Lab), Fudan University, Shanghai 200433, People's Republic of China
(Received 18 May 2003; published 16 March 2004)

We present experimental observations and numerical simulations of superlensing effect in liquid surface waves. We use rigid cylinders to create a two-dimensional periodic lattice, in which liquid surface waves propagate. Through the observation of a superlensing effect, we demonstrate the existence of negative refraction in surface waves. In addition, a complete band gap is found.

DOI: 10.1103/PhysRevE.69.030201 PACS number(s): 47.35.+i, 47.90.+a, 68.05.−n, 92.10.Hm

Wave refraction is a common phenomenon in daily life, occurring in classical waves such as electromagnetic waves, sonic waves, and liquid surface waves. In normal refraction, the incident and refracted waves stand on different sides of the normal direction of the interface between two media. However, it has been found recently that for electromagnetic waves two mechanisms can produce negative refraction [1] (now the refracted and incident waves lie on the same side of the interface normal), namely, plasmon resonance in metamaterials [2–4] and multiple Bragg scatterings in photonic crystals [5–8]. Experimental observations of negative refraction have been carried out for metamaterials [4,9,10] and photonic crystals [11] in microwaves.

In metamaterials [2–4] consisting of metallic wires and split rings, plasmon resonance may simultaneously lead to negative permittivity and permeability in a certain range of microwave frequencies [12,13], effectively producing a negative refractive index as a whole. When propagating in photonic crystals, electromagnetic waves are greatly modulated by multiple Bragg scatterings, leading to photonic band structures and photonic band gaps [14–16]. In photonic bands, the group and phase velocities may lie in different direction. This may lead to negative refraction in photonic crystals [5–8].

Can negative refraction occur in other kinds of classical waves, such as sonic or surface waves? In this paper, we will demonstrate theoretically and experimentally that negative refraction can also exist in liquid surface waves when propagating in a periodic structure. In addition, we find a complete band gap in liquid surface waves and confirm experimentally. To our best knowledge, the findings of negative refraction and complete band gap are made for the first time in surface waves.

Like electromagnetic waves in photonic crystals, liquid surface waves are also modulated by multiple Bragg scatterings when propagating in a periodic structure. Propagation of liquid surface waves is also characterized by band structures. Consequently, negative refraction may likewise occur in liquid surface waves. In metamaterials or photonic crystals, it is difficult to obtain experimentally the detailed information on the spatial wave patterns and the evolution of these patterns as a function of time. The advantage of using liquid surface waves lies in the fact that many interesting phenomena can be observed visually. We can observe not only the spatial distribution of wave patterns but also the time-dependent evolution of wave patterns. In fact, interesting phenomena, such as Bloch waves over a periodically drilled bottom, quasiperiodic Bloch-like waves over a quasiperiodically drilled bottom, and domain walls over a periodically drilled bottom with some disorder, have been observed in liquid surface wave experiments [17,18].

Pendry [19] suggested that negative refraction would lead to a superlensing effect: a point source placed in front of a flat rectangular slab that exhibits negative refraction would be refocused to form a real image on the opposite side of the slab. In particular, this superlens possesses several key advantages over conventional lenses, e.g., overcoming the diffraction limit. Experimental measurements in microwaves gave evidence that a flat rectangular slab of a metamaterial could focus power from a point source [10]. In addition, the superlensing effect was also demonstrated theoretically in photonic crystals [7]. Thus, the superlensing effect can serve as a criterion for judging the existence of negative refraction.

To demonstrate that negative refraction could also exist in liquid surface waves, we carry out a superlensing experiment in liquid surface waves. Our experimental setup is sketched in Fig. 1. A flat rectangular slab consisting of 202 circular copper cylinders is placed in the middle of a vessel which is horizontally placed. Copper cylinders are arranged in a square lattice. The side of the copper cylinder slab is (11) oriented. Copper cylinders with a height of 10 mm and diameter of 9 mm are mounted vertically onto a 2-mm-thick methacrylate plate. Along the (11) direction, there are nine rows of copper cylinders. The lattice constant of the square lattice is 10 mm. The vessel consists of a rectangular glass bottom adhered to a steel frame with four 10° slope wave-absorbing sides to minimize reflection from edges. The vessel is covered with a thin liquid with a depth of 6 mm. The chosen liquid has a very low capillary length to prevent the capillary effects [20]. The top of the vessel is covered by a glass lid in order to prevent liquid evaporation. A small vibrator serves as a point source generator. Both the amplitude and frequency of the vibrator can be tuned by a signal generator.

Figure 2(a) shows snapshots of three typical patterns of liquid surface waves projected onto the screen for different frequencies. The point source is placed on the left side of the slab, about 4 mm apart. On the left side of the slab, the

*Author to whom correspondence should be addressed; electronic address: jzi@fudan.edu.cn

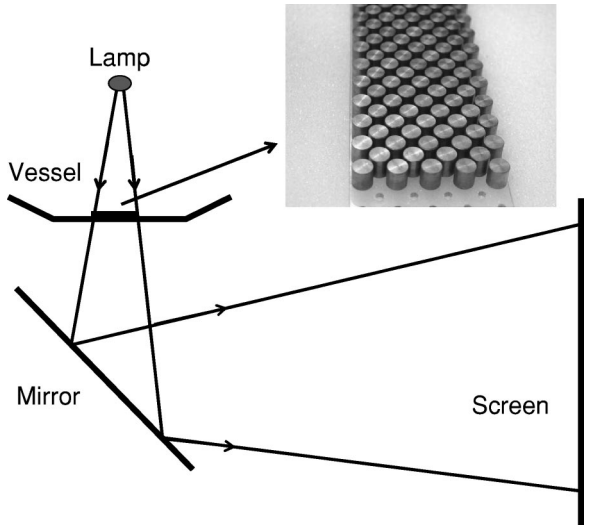

FIG. 1. Diagram of the experimental setup, consisting of a vessel, a flat rectangular slab of copper cylinders, a lamp, a mirror, and a screen. The rectangular slab of copper cylinders, shown as an inset, is placed in the middle of the vessel. A point source generator is placed on one side of the slab. A halogen lamp is hung above the vessel ($\sim$0.9 m). Enlarged liquid surface wave patterns can be seen on the screen (about 3.8 m apart from the mirror) with the help of the mirror placed below the vessel.

observed circlelike stripes show some distortions and within the same stripe there are some variations in brightness, owing to the interference between the source and the reflected wave. On the right side, the surface wave patterns change dramatically with frequency. For low frequencies, the transmitted wave patterns are circlelike, with their centers located inside the slab (left panel), i.e., forming a *virtual* image of the point source. With increasing frequency, this image shifts gradually to the right and eventually out of the slab. The middle panel shows that the image is outside the slab, i.e., forming a *real* image. Meanwhile, a backward-pointing conelike pattern is observed. With a further increase of the frequency, the image shifts further to the right and becomes elongated. In the meantime, a forward-pointing conelike pattern develops. Angles of both the forward- and backward-pointing conelike patterns decrease with the increasing frequency. Eventually, a nearly directive emission is produced (right panel). For frequencies above 8.2 Hz, no pattern is observable on the right side. We will show later that the pattern observed in the left panel corresponds to normal refraction, while that in the middle panel is a result of negative refraction.

To verify the experimental observations, numerical simulations are carried out for solving the liquid surface wave equation. For a harmonic mode with an angular frequency ω, the velocity potential Φ may be sought in the following form, based on the standard linearized wave theory for inviscid liquids [21,22]:

$$\Phi(x,y,z,t) = \mathrm{Re}[\phi(x,y)\cosh\kappa(z+h)e^{-i\omega t}], \qquad (1)$$

where z is the direction perpendicular to the bottom of the vessel and h is the liquid depth. ϕ is the solutions of the two-dimensional Helmholtz equation

$$(\nabla^2+\kappa^2)\phi = 0, \qquad (2)$$

where κ is the local wave number and can be obtained from the dispersion relation [17,18]

$$\omega^2 = g\kappa\tanh\kappa h(1+d_c^2\kappa^2), \qquad (3)$$

where g is the gravitational acceleration and d_c is the capillary length. The vertical displacement of the liquid surface η is related to ϕ by [21,22]

$$\eta(x,y,t) = \mathrm{Re}\left[-\frac{i\omega}{g}\phi(x,y)e^{-i\omega t}\right]. \qquad (4)$$

The Helmholtz equation can be solved on the framework of a multiple-scattering method [23]. The Helmholtz equation must be subjected to the boundary condition of no flow through the cylinder walls, namely, $\partial\phi/\partial\mathbf{n}=0$, where $\mathbf{n}$ is the direction normal to the surfaces of cylinders. The simulated patterns are shown in Fig. 2(b). Obviously, simulated results at the corresponding frequencies agree well with the experimental observations. From the theoretical results, we can obtain detailed information such as the spatial distributions of the surface waves, gaining a deeper insight into the interaction between the surface waves and the array of periodically arranged cylinders.

There have been intensive discussions of Bragg resonance in water waves in real spaces [24]. However, discussions of band structures in reciprocal space for liquid surface waves,

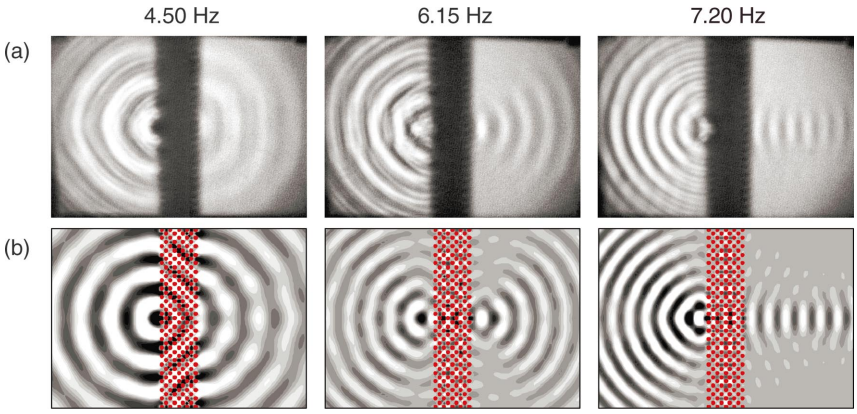

FIG. 2. (Color) Snapshots of liquid surface wave patterns. Dark and white represent positive and negative vibrations, respectively. (a) Experimentally observed patterns of liquid surface waves projected onto the screen. Black strip in the middle stands for the slab of copper cylinders. (b) Simulated results. Parameters used in simulations are the same as in experiment. Red dots denote copper cylinders.

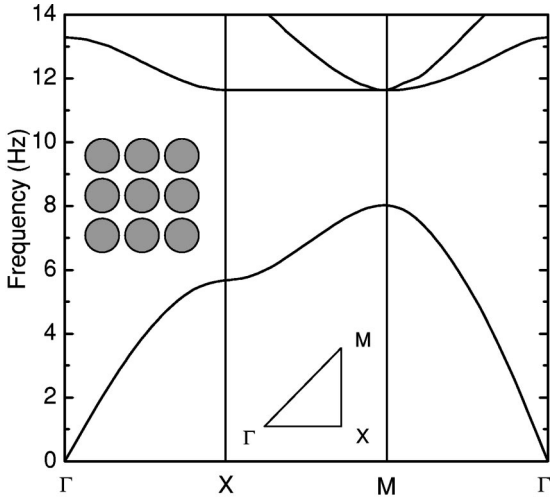

FIG. 3. Band structure for an infinite array of copper cylinders arranged in a square lattice. Parameters used in calculations are the same as in experiment. The array structure and the irreducible Brillouin zone are shown as insets. Γ, *X*, and *M* are the center, edge center, and corner of the first Brillouin zone, respectively.

as in solid state physics, are rare [23,25–28]. To account for the formation of the observed images, the band structure for liquid surface waves propagating through an infinite array of vertically arranged copper cylinders is calculated, also based on the multiple-scattering method [23] by applying the Bloch theorem to the liquid surface wave equation, shown in Fig. 3. A complete band gap opens up in the frequency range from 8.03 to 11.63 Hz, defined by the maximum of the first passing band at the *M* point and the minimum of the second passing band at the *M* point. The band gap is rather large, with the ratio of the gap width to the midgap frequency being 36.7%. As in photonic crystals, for frequencies within the band gap, propagation is forbidden in any direction. Propagation is, however, allowable for frequencies within the passing bands. Note that no complete band gaps in liquid surface waves have been found in previous experimental and theoretical studies [25–27].

Our discussions will be focused on the first passing band, at which the experiments are performed. Note that the energy flow direction is the same as the group velocity $\mathbf{v}_g = \nabla_k[\omega(k)]$, where the wave vector k is in the first Brillouin zone. It should be noted that the direction of the group velocity is given by the frequency-increasing direction normal to the constant-frequency contour (CFC), shown in Fig. 4(a). Thus, the refracted ray goes in the same direction as the group velocity $\mathbf{v}_g$. In the homogenous region without copper cylinders, the CFCs are all circles with the same center and their radius increases with the increasing frequency. In the region with copper cylinders, the situation is quite different. There exists a critical frequency of 5.75 Hz (the first passing band along the *XM* direction), at which the radius of curvature of the contours along the Γ*M* direction diverges. Below this critical frequency CFCs are centered at the Γ point and above it CFCs are centered at the *M* point. Near Γ or *M* points, the CFCs are circlelike, indicating an isotropic case. On the other hand, for frequencies near 5.75 Hz, a highly anisotropic case is expected.

After investigating the band structure, we consider refraction for an incident wave upon the interface between the regions with and without copper cylinders. The refracted

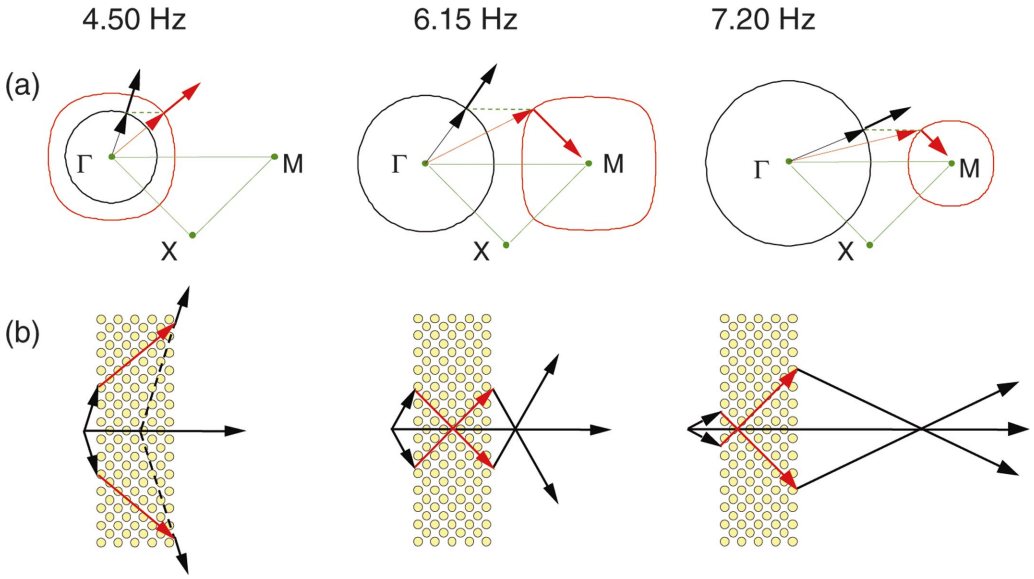

FIG. 4. (Color) (a) CFCs for different frequencies. Red and black curves stand for the CFCs in the regions with and without copper cylinders, respectively. Thin arrows denote the wave vectors, and thick arrows indicate the direction of the group velocity. Note that the interface between the regions with and without copper cylinders is perpendicular to the Γ*M* direction and the surface-parallel wave-vector component should be conserved in two media. (b) Diagram of refraction in the actual system. Each column represents the results for the corresponding frequencies shown on top of (a). Yellow dots denote copper cylinders. At 4.50 Hz, a virtual image is formed inside the slab of copper cylinders, corresponding to normal refraction. At 6.15 Hz, a real image is produced, resulting from negative refraction. At 7.20 Hz, a directive emission develops, although it still corresponds to negative refraction.

modes are determined by the conservation of the frequency and the wave-vector component parallel to the interface [5–7]. Using these criteria, we can determine the direction of the refracted wave, shown in Fig. 4(b). For frequencies below 5.75 Hz, normal refraction is expected, which corresponds to the case in the left panel of Fig. 2. For frequencies above 5.75 Hz, negative refraction occurs since the wave vector and the group velocity stand on the same side of the interface normal, which leads to what is observed in the middle panel of Fig. 2. Thus, the frequency of 5.75 Hz is a critical point, below (above) which normal (negative) refraction is expected. The experimentally observed critical frequency is about 5.8 Hz, in good agreement with the predicted one. For frequencies near the band edge, a directive emission on the right side of the slab is produced (right panel of Fig. 2), similar to that found in metamaterials [29]. For frequencies within the band gap, no waves can transmit. The band edge frequency, determined from experiment, is about 8.2 Hz, in good agreement with the predicted value of 8.03 Hz. From these analyses, we can conclude that the experimentally observed pattern in the middle panel of Fig. 2 is a result of negative refraction.

In summary, we have demonstrated the existence of negative refraction in liquid surface waves by a superlensing experiment and numerical simulations. In addition, a complete band gap for liquid surface waves is found for the first time. Our results pave the way for realizing many interesting phenomena caused by negative refraction since we can observe not only the spatial distributions but also the evolution of wave patterns. The interesting properties, such as negative refraction, directive emission, and band gap, render steering liquid surface waves and potential applications possible.

This work was supported mostly by Chinese National Key Basic Research Special Fund. Partial support from the National Science Foundation of China and from Shanghai Science and Technology Commission, China is acknowledged. We thank Dr. Z. Q. Qiu for a critical reading of the manuscript.

[1] V.G. Veselago, Usp. Fiz. Nauk. **92**, 517 (1967) [Sov. Phys. Usp. **10**, 509 (1968)].
[2] D.R. Smith, W.J. Padilla, D.C. Vier, S.C. Nemat-Nasser, and S. Schultz, Phys. Rev. Lett. **84**, 4184 (2000).
[3] R.A. Shelby, D.R. Smith, S.C. Nemat-Nasser, and S. Schultz, Appl. Phys. Lett. **78**, 489 (2001).
[4] R.A. Shelby, D.R. Smith, and S. Schultz, Science **292**, 77 (2001).
[5] M. Notomi, Phys. Rev. B **62**, 10696 (2000).
[6] B. Gralak, S. Enoch, and G. Tayeb, J. Opt. Soc. Am. A **17**, 1012 (2000).
[7] C. Luo, S.G. Johnson, J.D. Joannopoulos, and J.B. Pendry, Phys. Rev. B **65**, 201104 (2002).
[8] S. Foteinopoulou, E.N. Economou, and C.M. Soukoulis, Phys. Rev. Lett. **90**, 107402 (2003).
[9] C.G. Parazzoli, R.B. Greegor, K. Li, B.E.C. Koltenbah, and M. Tanielian, Phys. Rev. Lett. **90**, 107401 (2003).
[10] A.A. Houck, J.B. Brock, and I.L. Chuang, Phys. Rev. Lett. **90**, 137401 (2003).
[11] E. Cubukcu, K. Aydin, E. Ozbay, S. Foteinopoulou, and C.M. Soukoulis, Nature (London) **423**, 605 (2003).
[12] J.B. Pendry, A.J. Holden, W.J. Stewart, and I. Youngs, Phys. Rev. Lett. **76**, 4773 (1996).
[13] J.B. Pendry, A.J. Holden, D.J. Robbins, and W.J. Stewart, IEEE Trans. Microwave Theory Tech. **47**, 2075 (1999).
[14] E. Yablonovitch, Phys. Rev. Lett. **58**, 2059 (1987).
[15] S. John, Phys. Rev. Lett. **58**, 2486 (1987).
[16] J. D. Joannoupoulos, R. D. Meade, and J. N. Winn, *Photonic Crystals* (Princeton University Press, New York, 1995).
[17] M. Torres, J.P. Adrados, and F.M. de Espinosa, Nature (London) **398**, 114 (1999).
[18] M. Torres, J.P. Adrados, J.L. Aragón, P. Cobo, and S. Tehuacanero, Phys. Rev. Lett. **90**, 114501 (2003).
[19] J.B. Pendry, Phys. Rev. Lett. **85**, 3966 (2000).
[20] This liquid is CFC-113 of the Dupont company, a popular solvent with low viscosity $v=0.70\times10^{-2}$ cm^2/s, lower than that of water, a very low surface tension $T=17.3$ dyn/cm, and a high density $\rho=1.48$ g/cm^3. The capillary length of this liquid is $d_c=(T/\rho g)^{1/2}=1.09$ mm.
[21] C.-C. Mei, *The Applied Dynamics of Ocean Surface Waves* (World Scientific, Singapore, 1989).
[22] H. Lamb, *Hydrodynamics* (Cambridge University Press, Cambridge, 1995), p. 291.
[23] X. Hu, Y. Shen, X. Liu, R. Fu, J. Zi, X. Jiang, and S. Feng Phys. Rev. E **68**, 037301 (2003).
[24] C.C. Mei, J. Fluid Mech. **152**, 315 (1985); T. Hara and C.C. Mei, *ibid.* **178**, 221 (1987); C.C. Mei, T. Hara, and M. Naciri, *ibid.* **186**, 147 (1988); M. Naciri and C.C. Mei, *ibid.* **192**, 51 (1988); C.C. Mei and M. Naciri, Wave Motion **13**, 353 (1991).
[25] M. Torres, J.P. Adrados, F.R. Montero de Espinosa, D. García-Pablos, and J. Fayos, Phys. Rev. E **63**, 011204 (2001).
[26] T. Chou, J. Fluid Mech. **369**, 333 (1998).
[27] P. McIver, J. Fluid Mech. **424**, 101 (2000).
[28] X. Hu, Y. Shen, X. Liu, R. Fu, and J. Zi, Phys. Rev. E **68**, 066308 (2003).
[29] S. Enoch, G. Tayeb, P. Sabouroux, N. Guérin, and P. Vincent, Phys. Rev. Lett. **89**, 213902 (2002).